NIH Public Access
Author Manuscript
J Mol Cell Cardiol. Author manuscript; available in PMC 2015 September 01.

Published in final edited form as:
J Mol Cell Cardiol. 2014 September ; 74: 76–87. doi:10.1016/j.yjmcc.2014.04.020.

Ablation of Akt2 Protects against Lipopolysaccharide-Induced Cardiac Dysfunction: Role of Akt Ubiquitination E3 Ligase TRAF6

Yingmei Zhang[1,2,3,*], **Xihui Xu**[3,*], **Ceylan-Isik Asli**[3], **Maolong Dong**[3,5], **Zhaohui Pei**[4], **Yan Li**[1], and **Jun Ren**[2,3]

[1]Department of Cardiology, Fourth Military Medical University, Xi'an, China 710032

[2]Shanghai Institute of Cardiovascular Diseases, Zhongshan Hospital, Fudan University, Shanghai 200032, P.R. China

[3]Center for Cardiovascular Research and Alternative Medicine, University of Wyoming College of Health Sciences, Laramie, WY 82071, USA

[4]Department of Cardiology, The Third Hospital of Nanchang, Nanchang, Jiangxi 330009, China

[5]Department of Burn and Cutaneous Surgery Xijing Hospital, Fourth Military Medical University, Xi'an, China 710032

Abstract

Background—Lipopolysaccharide (LPS), an essential component of outer membrane of Gram-negative bacteria, plays a pivotal role in myocardial anomalies in sepsis. Recent evidence has depicted a role of Akt in LPS-induced cardiac sequelae although little information is available with regards to the contribution of Akt isoforms in the endotoxin-induced cardiac dysfunction. This study examined the effect of Akt2 knockout on LPS-induced myocardial contractile dysfunction and the underlying mechanism(s) with a focus on TNF receptor-associated factor 6 (TRAF6).

Methods—Echocardiographic and cardiomyocyte contractile function [peak shortening (PS), maximal velocity of shortening/ relengthening, time-to-PS, time-to-90% relengthening] were examined in wild-type and Akt2 knockout mice following LPS challenge (4 mg/kg, 4 hrs).

© 2014 Elsevier Ltd. All rights reserved.

Correspondence to: Dr. Jun Ren, Center for Cardiovascular Research and Alternative Medicine, University of Wyoming, College of Health Sciences, Laramie, WY 82071, USA, Tel: (307) 766-6131; Fax: (307) 766-2953, jren@uwyo.edu.
*Equal Contributions

Publisher's Disclaimer: This is a PDF file of an unedited manuscript that has been accepted for publication. As a service to our customers we are providing this early version of the manuscript. The manuscript will undergo copyediting, typesetting, and review of the resulting proof before it is published in its final citable form. Please note that during the production process errors may be discovered which could affect the content, and all legal disclaimers that apply to the journal pertain.

AUTHOR CONTRIBUTIONS
YZ, XX, AFC and MD collected researched data, ZP, YL and JR wrote manuscript.

CONFLICT OF INTERESTS
None declared.

NIH-PA Author Manuscript
NIH-PA Author Manuscript
NIH-PA Author Manuscript

NIH-PA Author Manuscript

NIH-PA Author Manuscript

NIH-PA Author Manuscript

Results—LPS challenge enlarged LV end systolic diameter, reduced fractional shortening and cardiomyocyte contractile capacity, prolonged TR_{90}, apoptosis, upregulated caspase-3/-12, ubiquitin, and the ubiquitination E3 ligase TRAF6 as well as decreased mitochondrial membrane potential without affecting the levels of TNF-α, toll-like receptor 4 and the mitochondrial protein ALDH2. Although Akt2 knockout failed to affect myocardial function, apoptosis, and ubiquitination, it significantly attenuated or mitigated LPS-induced changes in cardiac contractile and mitochondrial function, apoptosis and ubiquitination but not TRAF6. LPS facilitated ubiquitination, phosphorylation of Akt, GSK3β and p38, the effect of which with the exception of p38 was ablated by Akt2 knockout. TRAF6 inhibitory peptide or RNA silencing significantly attenuated LPS-induced Akt2 ubiquitination, cardiac contractile anomalies and apoptosis.

Conclusions—These data collectively suggested that TRAF6 may play a pivotal role in mediating LPS-induced cardiac injury via Akt2 ubiquitination.

Keywords

lipopolysaccharide; cardiac function; apoptosis; TRAF6; ubiquitination

INTRODUCTION

The bacterial endotoxin lipopolysaccharide (LPS) is deemed the principal culprit factor responsible for multi-organ failure including myocardial depression in sepsis [1–3]. The LPS-induced innate immune response is believed to be mediated through toll-like receptor-4 (TLR-4). Recognition of LPS by TLR4 usually triggers the recruitment of adaptors including MyD88, IL-1 receptor-associated kinases and TNF receptor-associated factor 6 (TRAF6) [4, 5], leading to the release of proinflammatory cytokines such as tumor necrosis factor α (TNF-α), interleukin (IL)-1β and IL-6 [6]. These proinflammatory cytokines may be responsible for LPS-induced multiple organ failure including heart failure [6, 7]. Up-to-date, a number of scenarios have been postulated for LPS-induced cardiac sequelae including decreased β-adrenergic sensitivity, elevated inducible nitric oxide synthase (iNOS), generation of reactive oxygen species (ROS), oxidative stress and activation of stress signaling including mitogen-activated protein kinase (MAPK), all of which prompt apoptotic cell death and myocardial dysfunction [7–10]. ROS is known to compromise mitochondrial integrity and cell survival through activation of essential stress signaling molecules including c-Jun N-terminal kinase (JNK) and p38 MAPK [11, 12]. Along the same line, recent eevidence from our lab suggested that LPS-induced myocardial depression may be attenuated by antioxidants including metallothionein and insulin-like growth factor I [13, 14]. Nonetheless, the precise mechanisms behind LPS-induced cardiac contractile dysfunction still remain elusive.

It has been documented that Akt may play a rather important role in LPS-induced cardiac responses [15, 16]. Akt serves as an essential cell survival signaling molecule with a pivotal role in cardiomyocyte survival and contractile homeostasis [17, 18]. While a number of studies have reported that beneficial outcome of Akt activation in the protection against sepsis-induced cardiac anomalies [19, 20], others have indicated a unique permissive role for PI3K/Akt in LPS-induced cardiac responses [21, 22]. Akt comprises three closely related isoforms namely Akt1, Akt2 and Akt3. Although these Akt proteins share high structural

NIH-PA Author Manuscript

NIH-PA Author Manuscript

NIH-PA Author Manuscript

and functional homology, genetic studies have suggested over-lapping although differential roles for these Akt isoforms in both physiological and pathophysiological settings [17]. Finding from our own laboratory has reported that Akt2 knockout is capable of protecting against high fat intake and NOS inhibition-induced cardiac contractile dysfunction [23, 24]. Nonetheless, the role of Akt isoform in LPS-induced cardiac anomalies remains unknown. To this end, this study was designed to examine the effect of Akt2 knockout on LPS-induced cardiac contractile dysfunction. Echocardiographic, cardiomyocyte contractile properties, and protein markers for apoptosis, inflammation (TNF-α and TLR4), mitochondrial integrity mitochondrial aldehyde dehydrogenase (ALDH2), ubiquitination (ubiquitin and the E3 ligase TRAF6), cell survival signaling Akt and GSK3β as well as the stress signaling molecules ERK, p38 and IκB were evaluated in adult wild-type and Akt2 knockout mice challenged with or without LPS. Recruitment of TRAF6 to the plasma membrane is necessary for TLR2- and TLR4-induced transactivation of NFκB and regulation of the subsequent pro-inflammatory response [25–27]. Deubiquitination of TRAF6 may be related to suppressed interleukin-6 production and inflammatory autoimmune diseases [27]. This E3 ligase is found to be essential to Akt ubiquitination [28]. TRAF6 synthesis has been shown to be induced at both mRNA and protein levels by LPS challenge [29]. Therefore, special attention was engaged towards the role for TRAF6 in LPS and Akt2 knockout-induced responses.

METHODS AND MATERIALS

Murine model of Akt2 knockout and LPS treatment

All animal procedures described here were in accordance with the Guide for the Care and Use of Laboratory Animals published by the US National Institutes of Health (NIH Publication No. 85-23, revised 1996) and were approved by the University of Wyoming Animal Care and Use Committee. The Akt2 knockout mice were obtained from Dr. Morris Birnbaum at the University of Pennsylvania (Philadelphia, PA) and were characterized previously [30]. In brief, Akt2 knockout and wild-type (WT) mice were housed in a pathogen-free environment. Mice were maintained with a 12/12-light/dark cycle with free access to regular rodent chow and tap water. On the day of experimentation, 4–5 month-old male WT and Akt2 knockout mice were injected intraperitoneally with 4 mg/kg *Escherichia Coli O55:B5* LPS dissolved in sterile saline or an equivalent volume of pathogenfree saline (vehicle groups). The dosage and duration (4 hrs) of LPS challenge was chosen based on earlier reports on the presence of myocardial dysfunction without significant mortality during the treatment period [13, 14, 31]. Four hours following LPS challenge, systolic and diastolic blood pressures were examined using a KODA semi-automated, amplified tail cuff device (Kent Scientific Corporation, Torrington, CT) (9, 9, 8 and 8 mice used for WT, WT-LPS, AKO and AKO-LPS groups, respectively).

Echocardiographic assessment

Four hrs after LPS challenge, cardiac geometry and function were evaluated in anesthetized (ketamine 80 mg/kg and xylazine 12 mg/kg, i.p.) mice using a 2-dimensional (2-D) guided M-mode echocardiography (Phillips Sonos 5500) equipped with a 15–6 MHz linear transducer (Phillips Medical Systems, Andover, MD). Adequate depth of anesthesia was

NIH-PA Author Manuscript

NIH-PA Author Manuscript

NIH-PA Author Manuscript

monitored using toe reflex. The heart was imaged in the 2-D mode in the parasternal long-axis view with a depth setting of 2 cm. The M-mode cursor was positioned perpendicular to interventricular septum and posterior wall of left ventricle (LV) at the level of papillary muscles from the 2-D mode. The sweep speed was 100 mm/s for the M-mode. Diastolic wall thickness, end diastolic dimension (EDD) and end systolic dimension (ESD) were measured. All measurements were done from leading edge to leading edge in accordance with the Guidelines of the American Society of Echocardiography [32]. The percentage of LV fractional shortening was calculated as [(EDD-ESD)/EDD] × 100. Heart rates were averaged from 10 cardiac cycles [33]. A total of 9, 9, 8 and 8 mice were used for WT, WT-LPS, AKO and AKO-LPS groups, respectively.

Isolation of cardiomyocytes

After ketamine/xylazine sedation, hearts were rapidly removed and mounted onto a temperature-controlled (37°C) Langendorff system. After perfusing with a modified Tyrode solution (Ca^{2+} free) for 2 min, the heart was digested for 20 min with 0.9 mg/ml Liberase Blendzyme 4 (Hoffmann-La Roche Inc., Indianapolis, IN) in a modified Tyrode solution. The modified Tyrode solution (pH 7.4) contained the following (in mM): NaCl 135, KCl 4.0, $MgCl_2$ 1.0, HEPES 10, NaH_2PO_4 0.33, glucose 10, butanedione monoxime 10, and the solution was gassed with 5% CO_2-95% O_2. The digested heart was then removed from the cannula and left ventricle was cut into small pieces in the modified Tyrode's solution. Tissue pieces were gently agitated and pellet of cells was resuspended. Extracellular Ca^{2+} was added incrementally back to 1.20 mM over a period of 30 min. Isolated cardiomyocytes were used for study within 8 hrs of isolation. Only rod-shaped cardiomyocytes with clear edges were selected for study [33].

Cell shortening/relengthening

Mechanical properties of cardiomyocytes were assessed using an IonOptix™ soft-edge system (IonOptix, Milton, MA). Cardiomyocytes were placed in a chamber mounted on the stage of an Olympus IX-70 microscope and superfused ~2 ml/min at 25°C) with a KHB buffer containing 1 mM $CaCl_2$. Myocytes were field stimulated at 0.5 Hz. Cell shortening and relengthening were assessed including peak shortening (PS), time-to-PS (TPS), time-to-90% relengthening (TR_{90}) and maximal velocities of shortening/relengthening (± dL/dt) [33]. To assess the role of TRAF6 in cardiomyocyte contractile function in response to LPS, cardiomyocytes were treated with LPS (1 μg/ml) for 4 hrs [34] in the absence or presence of the TRAF6 peptide inhibitor (DRQIKIWFQNRRMKWKK RKI PTE DEY, TRAF6 binding sequence underlined, IMG-2002, IMGEENEX, San Diego, CA) and control peptide (DRQIKIWFQNRRMKWKK, IMG-2002, IMGEENEX) (both at 300 μM) prior to mechanical assessment. A total of 35–37 cells were used from each mouse with a total of 4 mice being used per group.

Intracellular Ca^{2+} transient

Cardiomyocytes were loaded with fura-2/AM (0.5 μM) for 10min and fluorescence measurements were recorded with dual-excitation fluorescence photo multiplier system (Ionoptix). Cardiomyocytes were placed on an Olympus IX-70 inverted microscope and imaged through a Fluor 40× oil objective. Cells were exposed to light emitted by a 75-W

NIH-PA Author Manuscript

NIH-PA Author Manuscript

NIH-PA Author Manuscript

lamp and passed through either 360 nm or a 380 nm filter, while being stimulated to contract at 0.5Hz. Fluorescence emissions were detected between 480 nm and 520 nm by a photo multiplier tube after first illuminating the cells at a 360nm 0.5s, then at 380 nm for the duration of the recording protocol (333Hz sampling rate). The 360 nm excitation scan can be repeated at the end of the protocol and qualitative changes in intracellular Ca^{2+} concentration were inferred from the ratio of fura-2 fluorescence intensity at two wavelengths (360/380). Fluorescence decay time was assessed as an indication of intracellular Ca^{2+} clearing. Single and bi-exponential curve fit was applied to calculate the intracellular decay Ca^{2+} constant [33]. A total of 20 cells were used from each mouse with a total of 4 mice being used per group.

TUNEL assay

TUNEL staining of myonuclei positive for DNA strand breaks were determined using a fluorescence detection kit (Roche, Indianapolis, IN) and fluorescence microscopy. Briefly, paraffin-embedded sections (5 μm) were deparaffinized and rehydrated. The sections were then incubated with Proteinase K solution at room temperature for 30 min. TUNEL reaction mixture containing terminal deoxynucleotidyl transferase (TdT), fluorescein-dUTP was added to the sections in 50-μl drops and incubated for 60 min at 37°C in a humidified chamber in the dark. The sections were rinsed three times in PBS for 5 min each. Following embedding, sections were visualized with an Olympus BX-51 microscope equipped with an Olympus MaguaFire SP digital camera. DNase I and label solution were used as positive and negative controls. To determine the percentage of apoptotic cells, micrographs of TUNEL-positive and DAPI-stained nuclei were captured using an Olympus fluorescence microscope and counted using the ImageJ software (ImageJ version 1.43r; NIH) from 8–9 random fields at 400× magnification At least two hundred cells were counted in each field [35].

Measurement of mitochondrial membrane potential

Freshly isolated murine cardiomyocytes were suspended in HEPES-saline buffer and mitochondrial membrane potential ($\Delta\Psi_m$) was detected as described [36]. Briefly, after incubation with JC-1 (5 μM) for 10 min at 37°C, cells were rinsed twice by sedimentation using the HEPES saline buffer free of JC-1 before being examined under a confocal laser scanning microscope (Leica TCS SP2) at excitation wavelength of 490 nm. The emission of fluorescence was recorded at 530 nm (monomer form of JC-1, green) and at 590 nm (aggregate form of JC-1, red). Results in fluorescence intensity were expressed as 590-to-530-nm emission ratio.

RNA interference

Small interfering RNA (siRNA) against TRAF6 (On-TARGET plus SMART pool siRNA) or a non-targeting sequence was purchased from Dharmacon. The H9C2 cell cultures were transfected with siRNA (20 nM) in DMEM medium using the transfection reagent (DharmaFECT 1) following manufacturer's directions. Ninety-six hrs later, cells were challenged with LPS (1 μg/ml for 4 hrs).

NIH-PA Author Manuscript

NIH-PA Author Manuscript

NIH-PA Author Manuscript

Caspase-3 assay

Caspase-3 activity was measured as described [32]. Briefly, 1 ml PBS was added to a flask containing H9C2 myoblast homogenates prior to centrifugation at 10,000 *g* at 4°C for 10 min. The supernatant was discarded and homogenates were lysed in 100 μl of ice-cold cell lysis buffer [50 mM HEPES, pH 7.4, 0.1% CHAPS, 1 mM dithiothreitol (DTT), 0.1 mM EDTA, 0.1% NP40]. The assay was carried out in a 96-well plate with each well containing 30 μl of cell lysate, 70 μl of assay buffer (50 mM HEPES, 0.1% CHAPS, 100 mM NaCl, 10 mM DTT and 1 mM EDTA) and 20 μl of caspase-3 colorimetric substrate Ac-DEVDpNA (Sigma). The 96-well plate was incubated at 37°C for 1 hr, during which time the caspase in the sample was allowed to cleave the chromophore p-NA from the substrate molecule. Absorbency was detected at 405 nm with caspase-3 activity being proportional to color reaction. Protein content was determined using the Bradford method. The caspase-3 activity was expressed as picomoles of pNA released per μg of protein per min.

Western blot analysis

Myocardial protein was prepared as previously described [32]. Samples containing equal amount of proteins were separated on 10% SDS-polyacrylamide gels in a minigel apparatus (Mini-PROTEAN II, Bio-Rad, Hercules, CA)and transferred to nitrocellulose membranes. Membranes were blocked with 5% milk in TBS-T, and were incubated overnight at 4°C with anti-cleaved Caspase-3 (1:1,000, #9664, Cell Signaling Technology, Danvers, MA), anti-Caspase-12 (1:1,000, #2202 Cell Signaling), anti-TNF-α (1:1,000, #3707, Cell Signaling), anti-TLR4 (1:1,000, #2219, Cell Signaling), anti-ALDH2 (1:1,000, kindly provided by the late Dr. Henry Weiner, Purdue University, West Lafayette, IN), anti-TRAF6 (1:1000, #ab33915, Abcam, Cambridge, MA), anti-Ubiquitin (1:1,000, #ab7780, Abcam, Cambridge, MA), anti-Akt (1:1,000, #9272, Cell Signaling), anti-Akt1 (1:1,000, #2967, Cell Signaling), anti-Akt2 (1:1,000, #2962, Cell Signaling), anti-Akt3 (1:1,000, #3788, Cell Signaling), anti-phosphorylated Akt (pAkt, Ser473, 1:1,000, #4058, Cell Signaling), anti-GSK3β (1:1,000, #9315, Cell Signaling), anti-phosphorylated GSK3β (pGSK3β, Ser9, 1:1,000, #9323, Cell Signaling), anti-ERK (1:1,000, #9102, Cell Signaling), anti-phosphorylated ERK (pERK, Thr202/Tyr204, 1:1,000, #4377, Cell Signaling), anti-p38 (1:1,000, #9212, Cell Signaling), anti-phosphorylated (pp38, Thr180/Tyr182, 1:1,000, #9211, Cell Signaling), anti-IKB (1:1,000, #9242, Cell Signaling), anti-phosphorylated IKB (pIKB, Ser32, 1:1,000, #2859, Cell Signaling) and anti-GAPDH (1:1,000, loading control, #2118, Cell Signaling) antibodies. After immunoblotting, the film was scanned and the intensity of immunoblot bands was detected with a Bio-Rad Calibrated Densitometer.

Co-Immunoprecipitation (Co-IP)

Co-IP assay was performed with an anti-Akt antibody (Cell Signaling Technology, Danvers, MA) using a Pierce Co-Immunoprecipitation Kit (Thermo Scientific, Rockford, IL) according to the manufacturer's instruction. In brief, the Akt antibody (1: 100) was incubated with the AminoLink Plus coupling resin for 120 min at room temperature. After rinsing with coupling buffer, the resin was incubated with the cell lysate overnight at 4°C. Then, the resin was washed again with the IP washing buffer. Target protein complex was collected with elution buffer. A negative control that was provided with the IP kit was

NIH-PA Author Manuscript

NIH-PA Author Manuscript

NIH-PA Author Manuscript

employed as the negative control. Collected samples were analyzed using Western blot to detect the levels of Akt1, Akt2 and ubiquitin [37]. Next, reverse Co-IP was performed following the same procedure to pull down ubiquitinated proteins. In the samples pulled down with ubiquitin antibody, expression of Akt1 and Akt2 was examined using Western blot analysis.

Statistical analysis

Mean ± SEM. Statistical significance ($p < 0.05$) for each variable was estimated by one-way analysis of variance (ANOVA) followed by Tukey's post hoc test where appropriate.

RESULTS

General features and echocardiographic properties of WT and Akt2 knockout mice with or without LPS challenge

LPS challenge did not overtly affect body, heart, liver and kidney weights in WT or Akt2 knockout mice. Akt2 knockout did not affect body or organ weights. Systolic and diastolic blood pressure, heart rate, LV wall thickness, LV EDD and LV mass were comparable among all groups. LPS challenge significantly increased LV ESD and reduced fractional shortening in WT mice, the effect of which was ablated by Akt2 knockout. Akt2 knockout itself did not affect any of the echocardiographic indices tested (Table 1).

Effect of Akt2 knockout on LPS-induced cardiomyocyte contractile and intracellular Ca^{2+} responses

Neither LPS challenge nor Akt2 knockout affected the overall appearance of murine cardiomyocytes (supplemental Fig. S1). Assessment of cardiomyocyte contractile function revealed little difference in resting cell length between WT and Akt2 knockout mice in the absence of LPS treatment. As expected, LPS challenge significantly reduced PS, ± dL/dt, prolonged TR_{90} without affecting TPS. Akt2 knockout itself did not affect cardiomyocyte mechanical indices although it overtly attenuated or abrogated LPS-induced cardiomyocyte mechanical defects (Fig. 1). To better understand the mechanism(s) behind Akt knockout-offered beneficial effect, fura-2 fluorescence was monitored to evaluate intracellular Ca^{2+} handling. Cardiomyocytes from LPS-challenged WT mice displayed reduced intracellular Ca^{2+} release in response to electrical stimuli (ΔFFI) and prolonged intracellular Ca^{2+} decay (single but not bi-exponential curve fitting) along with unchanged resting intracellular Ca^{2+} (resting FFI), the effect of which was reconciled by Akt knockout. Akt knockout itself did not alter intracellular Ca^{2+} homeostasis (Fig. 2).

Effect of Akt2 knockout on LPS-induced changes in apoptosis, inflammation, mitochondrial membrane potential, mitochondrial integrity and ubiquitination

To examine the mechanism(s) of action behind Akt2 knockout-elicited protective effect against LPS-induced myocardial dysfunction, TUNEL staining, protein markers for apoptosis, inflammation, mitochondrial integrity and ubiquitination were examined. Our data depicted that LPS challenge promoted myocardial apoptosis (as shown by percent TUNEL positive cells) and loss of cardiomyocyte mitochondrial membrane potential. Although Akt2 knockout itself did not affect cardiac apoptosis and mitochondrial membrane

NIH-PA Author Manuscript

NIH-PA Author Manuscript

NIH-PA Author Manuscript

potential, it mitigated LPS-induced changes in apoptosis and mitochondrial membrane integrity (Fig. 3). Consistently, our data revealed that LPS upregulated pro-apoptotic markers caspase-3/-12, the ubiquitination protein ubiquitin and the ubiquitination E3 ligase TRAF6. Although Akt2 knockout did not affect myocardial apoptosis, inflammation, mitochondrial integrity and ubiquitination, it ablated LPS-induced changes in caspase-3/-12 and ubiquitin without affecting LPS-induced increase in TRAF6. Neither Akt2 knockout nor LPS challenge, or both, affected the levels of proinflammatory proteins TNF-α and TLR4 as well as the mitochondrial protein ALDH2 (Fig. 4).

Role of Akt2 knockout on LPS-induced changes in Akt, GSK3β and stress signaling activation

To examine the possible role of signaling mechanisms for cell survival and stress in Akt2 knockout- and LPS-induced myocardial responses, activation of the cell survival signal Akt and its downstream signal GSK3β as well as the stress signaling molecules ERK, p38 and IΚB were examined in WT and Akt2 knockout mice treated with or without LPS. Our data shown in Fig. 5 and Fig. 6 depicted that LPS treatment significantly enhanced phosphorylation of Akt, GSK3β and p38 without affecting that of ERK and IΚB. Akt2 knockout significantly decreased the pan and phosphorylated Akt. Although Akt2 knockout itself failed to affect the pan and phosphorylated protein expression of GSK3β, ERK, p38 and IΚB, it nullified LPS-induced activation of Akt and GSK3β without affecting that of the stress signaling cascades (ERK, p38 and IΚB). LPS challenge did not overtly affect pan protein expression of Akt, GSK3β, ERK, p38 and IΚB. Our result further revealed complete deletion of Akt2 isoform by Akt2 knockout, validating the murine model. LPS did not alter the protein expression of Akt2 isoform. Neither LPS challenge nor Akt2 knockout overtly affected the levels of Akt1 and Akt3 isoforms (supplemental Fig. S2).

Effect of inhibition of TRAF6 on LPS-induced changes in cardiomyocyte mechanics

To further examine the role of TRAF6 in LPS-induced cardiomyocyte contractile defects, freshly isolated cardiomyocytes from WT and Akt2 knockout mice were challenge with LPS (1 μg/ml) for 4 hrs in the absence or presence of the TRAF6 peptide inhibitor or control peptide (300 μM). In line with the *in vivo* findings, LPS significantly decreased PS and ± dL/dt as well as prolonged TR_{90} without affecting resting cell length and TPS, the effects of which were abolished by TRAF6 peptide inhibitor and Akt2 knockout without any additive effect between the two. The control peptide failed to affect LPS-induced cardiomyocyte mechanical defects. Neither TRAF6 peptide inhibitor nor control peptide affected cardiomyocyte contractile properties themselves (Fig. 7). These data provided evidence for a role of the E3 ligase TRAF6 and Akt2 in LPS-induced cardiac contractile anomalies.

Effect of siRNA silence of TRAF6 on LPS-induced changes in apoptosis and Akt

To further consolidate a role of TRAF6 in LPS-induced cell survival and regulation of Akt activation, H9C2 myoblasts were transfected with siRNA to silence TRAF6 prior to challenge with LPS (1 μg/ml) for 4 hrs. Our data shown in Fig. 8 revealed that knockdown of TRAF6 ablated LPS-induced apoptosis (at 2-, 4- and 8-hrs of exposure) and Akt

NIH-PA Author Manuscript

NIH-PA Author Manuscript

NIH-PA Author Manuscript

phosphorylation without eliciting any over effect by TRAF6 silencing itself. These data support a role of TRAF6 in LPS-induced cell death and Akt activation.

TRAF6 and Akt2 mediate LPS-induced Akt ubiquitination

Given the role of TRAF6 in the regulation of Akt ubiquitination [28], we examined the role of TRAF6 in LPS-induced Akt ubiquitination, if any, using the co-immunoprecipitation technique. Cardiomyocytes from WT and Akt2 knockout mice were challenge with LPS (1 μg/ml) for 4 hrs in the absence or presence of the TRAF6 peptide inhibitor or control peptide (300 μM) prior to immunoblotting analysis. Following direct immunoprecipitation (IP) for pan Akt, levels of Akt1 were found to be similar in WT or Akt2 knockout groups with or without LPS or TRAF inhibitor treatment (Fig. 9A, B). Furthermore, our co-IP results revealed that LPS dramatically increased Akt ubiquitination, the effect of which was ablated by TRAF6 inhibitor and Akt2 knockout (Fig. 9A, C). Moreover, basal level of Akt ubiquitination was dramatically decreased in response to Akt2 depletion. To further confirm these co-IP findings, a reverse co-IP was performed to pull down the ubiquitinated proteins prior to probing for Akt isoforms. LPS challenge was found to dramatically increase the level of ubiquitinated Akt2, the effect of which was ablated by TRAF6 peptide inhibitor. Interestingly, little Akt1 was pulled down with ubiquitinated proteins in the reverse co-IP experiment (Fig. 9D, E). These data suggested that LPS challenge significantly promoted Akt2 (but not Akt1) ubiquitination through regulation of TRAF6.

DISCUSSION

The salient findings from our study depicted that Akt2 knockout rescued LPS-induced cardiac contractile dysfunction, intracellular Ca^{2+} mishandling, mitochondrial injury and apoptosis. The beneficial effects of Akt2 knockout against LPS-induced myocardial anomalies appear to be mediated through inhibition of the E3 ligase TRAF6-mediated Akt2 (but not Akt1) ubiquitination. Furthermore, Akt2 knockout alleviated LPS-induced phosphorylation of Akt and GSK3β but not p38 phosphorylation. Our *in vitro* study consolidated the causative relationship of TRAF6 and LPS-elicited cardiac anomalies. Our results did not favor a predominant role for pro-inflammatory signaling and mitochondrial protein (ALDH2) in the Akt2 knockout-elicited cardioprotection against LPS. These findings implicate beneficial role of Akt2 knockout against LPS-induced myocardial anomalies possibly through a TRAF-6-dependent Akt2 ubiquitination. Given that Akt2 knockout itself did not alter cardiac contractile function and cell survival in the absence of endotoxin exposure, its beneficial role against LPS-induced cardiac dysfunction and apoptosis suggests the potential of Akt2 as a therapeutic target in the clinical management of cardiovascular complication in sepsis.

Sepsis is a serious clinical problem with rather high mortality [38]. Compromised cardiac contractile function is common in sepsis [13, 14, 31, 39]. LPS, the major component of bacterial outer membrane, plays an important role in the pathogenesis of cardiac anomalies in sepsis [8]. Data from our study revealed reduced fractional shortening, PS and ± dL/dt, prolongation of TR_{90} following LPS challenge, in line with earlier reports [32, 33, 40]. The echocardiographic observation of a decreased fractional shortening in LPS-treated mice is

NIH-PA Author Manuscript

NIH-PA Author Manuscript

NIH-PA Author Manuscript

likely attributed to enlarged LVESD along with unchanged LVEDD, symbolizing compromised systolic function. The fact that Akt2 knockout alleviated LPS-induced cardiac contractile and intracellular Ca^{2+} derangement, apoptosis, mitochondrial injury and activation of Akt and GSK3β favors a role of lessened phosphorylation of Akt and its downstream signal GSK3β in Akt2 knockout-elicited cardiac injury. The observation that Akt2 knockout failed to alter cardiac mechanical function and cell survival possibly suggests that Akt2 knockout itself may not be innately harmful to the heart. We did not note any major changes in the levels of Akt1 and Akt3 in LPS- or Akt2 depleted mice, not favoring compensatory regulation from other Akt isoforms (Akt1 and Akt3). Possible involvement of Akt1 in LPS-induced anomalies was also denied by the co-IP (reverse co-IP) experiments where Akt1 isoform was unlikely to be ubiquitinated (only a rather faint band was noted for Akt3 in the heart as shown in Fig. S2). Oxidative stress and stress signaling activation have been demonstrated in sepsis-induced organ dysfunction in particular myocardial anomalies [7, 40, 41]. In our hands, LPS-induced elevation of p38 MAPK phosphorylation was unaffected by Akt2 knockout, not favoring a role of stress signaling regulation in Akt2 knockout-elicited cardioprotection against LPS exposure.

Although our study favors a beneficial role of Akt2 knockout in LPS-induced cardiac contractile dysfunction, intracellular Ca^{2+} defect and apoptosis, convincing clinical evidence regarding a role of Akt in heart failure in sepsis is still lacking. Our data revealed that Akt2 knockout protected against LPS-induced cardiac apoptosis and loss of mitochondrial membrane potential, in line with the notion that mitochondrial injury contributes to cardiac dysfunction in sepsis [42]. Nonetheless, data from our study did not favor a major role of mitochondrial chaperone protein ALDH2 in the Akt2 knockout-elicited beneficial effect against cardiac contractile anomalies and apoptosis in sepsis.

TRAF6 has been identified as a ligase for Akt ubiquitination and membrane recruitment and its phosphorylation on growth factor stimulation [28]. Findings from our study revealed that TRAF6 peptide inhibitor or siRNA knockdown (but not non-target RNA) alleviated or ablated LPS-induced contractile anomalies, apoptosis and Akt activation, indicating a role of TRAF6 in LPS-induced cell injury. Inhibition of TRAF6 using RNA silence or decoy peptides decreases tumor cell proliferation and promotes apoptosis [26, 27, 43] although insufficient information is available with regards to the role of TRAF6 in heart failure. Ubiquitination, an essential component of the ubiquitin-proteasome system (UPS), is a cell degradation machinery through which mammalian cells degrade and recycle macromolecules and organelles [44]. Enhanced myocardial ubiquitination has been reported in various cardiovascular diseases including sepsis [29, 44]. Inhibition of Akt ubiquitination has been reported to suppress Akt phosphorylation [28], indicating that TRAF6 may promote Akt phosphorylation by way of Akt2 ubiquitination. Data from our study suggest enhanced Akt2 but not Akt1 ubiquitination in association with cardiac contractile and intracellular Ca^{2+} abnormalities and apoptosis in response to LPS challenge (depicted in the scheme from Fig. 10), consistent with the notion that ubiquitination may be upregulated under cell stress [45]. Our results strongly favor a role of ubiquitination and subsequent Akt phosphorylation in Akt2 knockout-elicited cardioprotection. Further scrutiny is warranted to better understand the sequential cellular event of ubiquitination-phosphorylation as well as protein quality control in myocardial dysfunction under sepsis.

NIH-PA Author Manuscript

NIH-PA Author Manuscript

NIH-PA Author Manuscript

In conclusion, findings from our current study revealed that Akt2 may be the crucial Akt isoform mediating LPS-induced cardiac sequelae under sepsis. Akt2 knockout is capable of rescuing LPS-induced cardiac contractile defect, intracellular Ca^{2+} mishandling, apoptosis and mitochondrial injury possibly through interruption of TRAF6-mediated Akt2 ubiquitination and activation. These findings have shed some lights towards the understanding for a pivotal role of ubiquitination in endotoxemia-induced myocardial injury. Furthermore, our study has revealed the clinical value of Akt2 and TRAF6 (as well as ubiquitination) as potential therapeutic targets in the management of heart failure in sepsis. Given that TRAF6 may also be ubiquitinated to govern TLR4-triggered autophagic cell injury [46], further study should focus on the interplay between protein quality control (e.g., autophagy and ubiquitination) and myocardial contractile function in the face of sepsis.

Supplementary Material

Refer to Web version on PubMed Central for supplementary material.

Acknowledgments

FUNDING SOURCES

This work was supported in part by NIH/NCRR P20 RR016474 and GM103432.

REFERENCE

1. Angus DC, Pereira CA, Silva E. Epidemiology of severe sepsis around the world. Endocr Metab Immune Disord Drug Targets. 2006; 6:207–212. [PubMed: 16787296]
2. Angus DC, Wax RS. Epidemiology of sepsis: an update. Crit Care Med. 2001; 29:S109–S116. [PubMed: 11445744]
3. Opal SM, Scannon PJ, Vincent JL, et al. Relationship between plasma levels of lipopolysaccharide (LPS) and LPS-binding protein in patients with severe sepsis and septic shock. J Infect Dis. 1999; 180:1584–1549. [PubMed: 10515819]
4. Lin XW, Xu WC, Luo JG, et al. WW Domain Containing E3 Ubiquitin Protein Ligase 1 (WWP1) Negatively Regulates TLR4-Mediated TNF-alpha and IL-6 Production by Proteasomal Degradation of TNF Receptor Associated Factor 6 (TRAF6). PloS one. 2013; 8:e67633. [PubMed: 23799152]
5. Medzhitov R, Preston-Hurlburt P, Kopp E, et al. MyD88 is an adaptor protein in the hToll/IL-1 receptor family signaling pathways. Molecular cell. 1998; 2:253–258. [PubMed: 9734363]
6. Ward PA. The sepsis seesaw: seeking a heart salve. Nat Med. 2009; 15:497–498. [PubMed: 19424210]
7. Ren J, Wu S. A burning issue: do sepsis and systemic inflammatory response syndrome (SIRS) directly contribute to cardiac dysfunction? Front Biosci. 2006; 11:15–22. [PubMed: 16146710]
8. Yasuda S, Lew WY. Lipopolysaccharide depresses cardiac contractility and beta-adrenergic contractile response by decreasing myofilament response to Ca2+ in cardiac myocytes. Circ Res. 1997; 81:1011–1020. [PubMed: 9400382]
9. Zhang WJ, Wei H, Frei B. Genetic deficiency of NADPH oxidase does not diminish, but rather enhances, LPS-induced acute inflammatory responses in vivo. Free radical biology & medicine. 2009; 46:791–798. [PubMed: 19124074]
10. Ben-Shaul V, Lomnitski L, Nyska A, Zurovsky Y, Bergman M, Grossman S. The effect of natural antioxidants, NAO and apocynin, on oxidative stress in the rat heart following LPS challenge. Toxicol Lett. 2001; 123:1–10. [PubMed: 11514100]
11. Fiers W, Beyaert R, Declercq W, Vandenabeele P. More than one way to die: apoptosis, necrosis and reactive oxygen damage. Oncogene. 1999; 18:7719–7730. [PubMed: 10618712]

NIH-PA Author Manuscript

NIH-PA Author Manuscript

NIH-PA Author Manuscript

12. Sakon S, Xue X, Takekawa M, et al. NF-kappaB inhibits TNF-induced accumulation of ROS that mediate prolonged MAPK activation and necrotic cell death. EMBO J. 2003; 22:3898–3909. [PubMed: 12881424]

13. Ceylan-Isik AF, Zhao P, Zhang B, Xiao X, Su G, Ren J. Cardiac overexpression of metallothionein rescues cardiac contractile dysfunction and endoplasmic reticulum stress but not autophagy in sepsis. Journal of molecular and cellular cardiology. 2010; 48:367–378. [PubMed: 19914257]

14. Zhao P, Turdi S, Dong F, et al. Cardiac-specific overexpression of insulin-like growth factor I (IGF-1) rescues lipopolysaccharide-induced cardiac dysfunction and activation of stress signaling in murine cardiomyocytes. Shock. 2009; 32:100–107. [PubMed: 18948844]

15. Yao YW, Zhang GH, Zhang YY, et al. Lipopolysaccharide pretreatment protects against ischemia/reperfusion injury via increase of HSP70 and inhibition of NF-kappaB. Cell Stress Chaperones. 2011; 16:287–296. [PubMed: 21080136]

16. Hotchkiss RS, Karl IE. The pathophysiology and treatment of sepsis. N Engl J Med. 2003; 348:138–150. [PubMed: 12519925]

17. Hers I, Vincent EE, Tavare JM. Akt signalling in health and disease. Cellular signalling. 2011; 23:1515–1527. [PubMed: 21620960]

18. Zhang Y, Xia Z, La Cour KH, Ren J. Activation of Akt rescues endoplasmic reticulum stress-impaired murine cardiac contractile function via glycogen synthase kinase-3beta-mediated suppression of mitochondrial permeation pore opening. Antioxid Redox Signal. 2011; 15:2407–2424. [PubMed: 21542787]

19. Dong M, Hu N, Hua Y, et al. Chronic Akt activation attenuated lipopolysaccharide-induced cardiac dysfunction via Akt/GSK3beta-dependent inhibition of apoptosis and ER stress. Biochimica et biophysica acta. 2013; 1832:848–863. [PubMed: 23474308]

20. Jiang S, Zhu W, Li C, et al. alpha-Lipoic acid attenuates LPS-induced cardiac dysfunction through a PI3K/Akt-dependent mechanism. International immunopharmacology. 2013; 16:100–107. [PubMed: 23562296]

21. Ha T, Hua F, Liu X, et al. Lipopolysaccharide-induced myocardial protection against ischaemia/reperfusion injury is mediated through a PI3K/Akt-dependent mechanism. Cardiovascular research. 2008; 78:546–553. [PubMed: 18267957]

22. Yao Y, Zhang F, Wang L, et al. Lipopolysaccharide preconditioning enhances the efficacy of mesenchymal stem cells transplantation in a rat model of acute myocardial infarction. Journal of biomedical science. 2009; 16:74. [PubMed: 19691857]

23. Roe ND, Ren J. Akt2 knockout mitigates chronic iNOS inhibition-induced cardiomyocyte atrophy and contractile dysfunction despite persistent insulin resistance. Toxicol Lett. 2011; 207:222–231. [PubMed: 21964073]

24. Xu X, Hua Y, Nair S, Zhang Y, Ren J. Akt2 knockout preserves cardiac function in high-fat diet-induced obesity by rescuing cardiac autophagosome maturation. Journal of molecular cell biology. 2013; 5:61–63. [PubMed: 23258696]

25. Verstak B, Nagpal K, Bottomley SP, Golenbock DT, Hertzog PJ, Mansell A. MyD88 adapter-like (Mal)/TIRAP interaction with TRAF6 is critical for TLR2- and TLR4-mediated NF-kappaB proinflammatory responses. The Journal of biological chemistry. 2009; 284:24192–24203. [PubMed: 19592497]

26. Ma J, Bang BR, Lu J, et al. The TNF family member 4-1BBL sustains inflammation by interacting with TLR signaling components during late-phase activation. Science signaling. 2013; 6:ra87. [PubMed: 24084649]

27. Xia M, Liu J, Wu X, et al. Histone methyltransferase Ash1l suppresses interleukin-6 production and inflammatory autoimmune diseases by inducing the ubiquitin-editing enzyme A20. Immunity. 2013; 39:470–481. [PubMed: 24012418]

28. Yang WL, Wang J, Chan CH, et al. The E3 ligase TRAF6 regulates Akt ubiquitination and activation. Science. 2009; 325:1134–1138. [PubMed: 19713527]

29. Jakus PB, Kalman N, Antus C, et al. TRAF6 is functional in inhibition of TLR4-mediated NF-kappaB activation by resveratrol. J Nutr Biochem. 2012

30. Cho H, Mu J, Kim JK, et al. Insulin resistance and a diabetes mellitus-like syndrome in mice lacking the protein kinase Akt2 (PKB beta). Science. 2001; 292:1728–1731. [PubMed: 11387480]

NIH-PA Author Manuscript

NIH-PA Author Manuscript

NIH-PA Author Manuscript

31. Peng T, Lu X, Feng Q. Pivotal role of gp91phox-containing NADH oxidase in lipopolysaccharide-induced tumor necrosis factor-alpha expression and myocardial depression. Circulation. 2005; 111:1637–1644. [PubMed: 15795323]
32. Manning WJ, Wei JY, Katz SE, Litwin SE, Douglas PS. In vivo assessment of LV mass in mice using high-frequency cardiac ultrasound: necropsy validation. Am J Physiol. 1994; 266:H1672–H1675. [PubMed: 8184946]
33. Doser TA, Turdi S, Thomas DP, Epstein PN, Li SY, Ren J. Transgenic overexpression of aldehyde dehydrogenase-2 rescues chronic alcohol intake-induced myocardial hypertrophy and contractile dysfunction. Circulation. 2009; 119:1941–1949. [PubMed: 19332462]
34. Cheng YC, Chen LM, Chang MH, et al. Lipopolysaccharide upregulates uPA, MMP-2 and MMP-9 via ERK1/2 signaling in H9c2 cardiomyoblast cells. Mol Cell Biochem. 2009; 325:15–23. [PubMed: 19184369]
35. Zhang B, Turdi S, Li Q, et al. Cardiac overexpression of insulin-like growth factor 1 attenuates chronic alcohol intake-induced myocardial contractile dysfunction but not hypertrophy: Roles of Akt, mTOR, GSK3beta, and PTEN. Free radical biology & medicine. 2010; 49:1238–1253. [PubMed: 20678571]
36. Zhang Y, Babcock SA, Hu N, Maris JR, Wang H, Ren J. Mitochondrial aldehyde dehydrogenase (ALDH2) protects against streptozotocin-induced diabetic cardiomyopathy: role of GSK3beta and mitochondrial function. BMC medicine. 2012; 10:40. [PubMed: 22524197]
37. Adebiyi A, Narayanan D, Jaggar JH. Caveolin-1 assembles type 1 inositol 1,4,5-trisphosphate receptors and canonical transient receptor potential 3 channels into a functional signaling complex in arterial smooth muscle cells. The Journal of biological chemistry. 2011; 286:4341–4348. [PubMed: 21098487]
38. Rivers E, Nguyen B, Havstad S, et al. Early goal-directed therapy in the treatment of severe sepsis and septic shock. N Engl J Med. 2001; 345:1368–1377. [PubMed: 11794169]
39. Niederbichler AD, Westfall MV, Su GL, et al. Cardiomyocyte function after burn injury and lipopolysaccharide exposure: single-cell contraction analysis and cytokine secretion profile. Shock. 2006; 25:176–183. [PubMed: 16525357]
40. Ren J, Ren BH, Sharma AC. Sepsis-induced depressed contractile function of isolated ventricular myocytes is due to altered calcium transient properties. Shock. 2002; 18:285–288. [PubMed: 12353932]
41. Obata T, Brown GE, Yaffe MB. MAP kinase pathways activated by stress: the p38 MAPK pathway. Crit Care Med. 2000; 28:N67–N77. [PubMed: 10807318]
42. Joshi MS, Julian MW, Huff JE, Bauer JA, Xia Y, Crouser ED. Calcineurin regulates myocardial function during acute endotoxemia. Am J Respir Crit Care Med. 2006; 173:999–1007. [PubMed: 16424445]
43. Liu H, Tamashiro S, Baritaki S, et al. TRAF6 activation in multiple myeloma: a potential therapeutic target. Clinical lymphoma, myeloma & leukemia. 2012; 12:155–163.
44. Cui Z, Scruggs SB, Gilda JE, Ping P, Gomes AV. Regulation of cardiac proteasomes by ubiquitination, SUMOylation, and beyond. Journal of molecular and cellular cardiology. 2013
45. Sixt SU, Dahlmann B. Extracellular, circulating proteasomes and ubiquitin - incidence and relevance. Biochimica et biophysica acta. 2008; 1782:817–823. [PubMed: 18602990]
46. Zhan Z, Xie X, Cao H, et al. Autophagy facilitates TLR4- and TLR3-triggered migration and invasion of lung cancer cells through the promotion of TRAF6 ubiquitination. Autophagy. 2014; 10:257–268. [PubMed: 24321786]

NIH-PA Author Manuscript

NIH-PA Author Manuscript

NIH-PA Author Manuscript

Highlights

- Lipopolysaccharide induces cardiac anomalies, elevated TRAF6 and Akt2 ubiquitination;
- Akt2 knockout alleviates LPS-induced changes in cardiac function and apoptosis;
- Akt2 knockout-induced protection is mediated via suppression of TRAF6-mediated Akt2 ubiquitination;

NIH-PA Author Manuscript
NIH-PA Author Manuscript
NIH-PA Author Manuscript

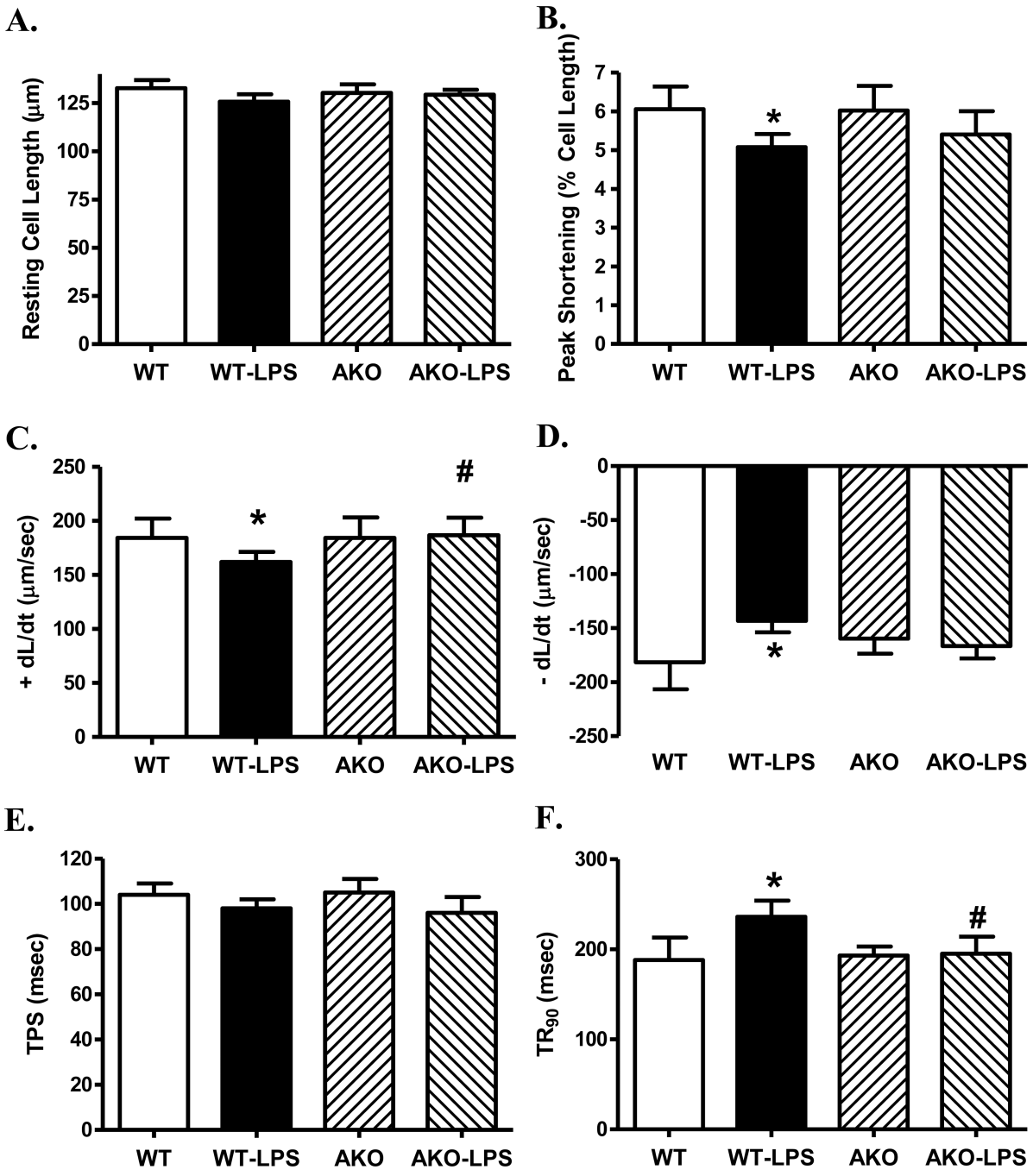

Fig. 1.

Cardiomyocyte contractile properties in WT and Akt2 knockout (AKO) mice treated with LPS (4 mg/kg, i.p.) or saline for 4 hrs. A: Resting cell length; B: Peak shortening (normalized to cell length); C: Maximal velocity of shortening (+ dL/dt); D: Maximal velocity of relengthening (−dL/dt); E: Time-to-peak shortening (TPS); and F: Time-to-90% relengthening (TR_{90}). Mean ± SEM, n = 4 mice (35–37 cells per mouse) per group; * $p < 0.05$ *vs*. WT group, # $p < 0.05$ *vs*. WT-LPS group.

NIH-PA Author Manuscript
NIH-PA Author Manuscript
NIH-PA Author Manuscript

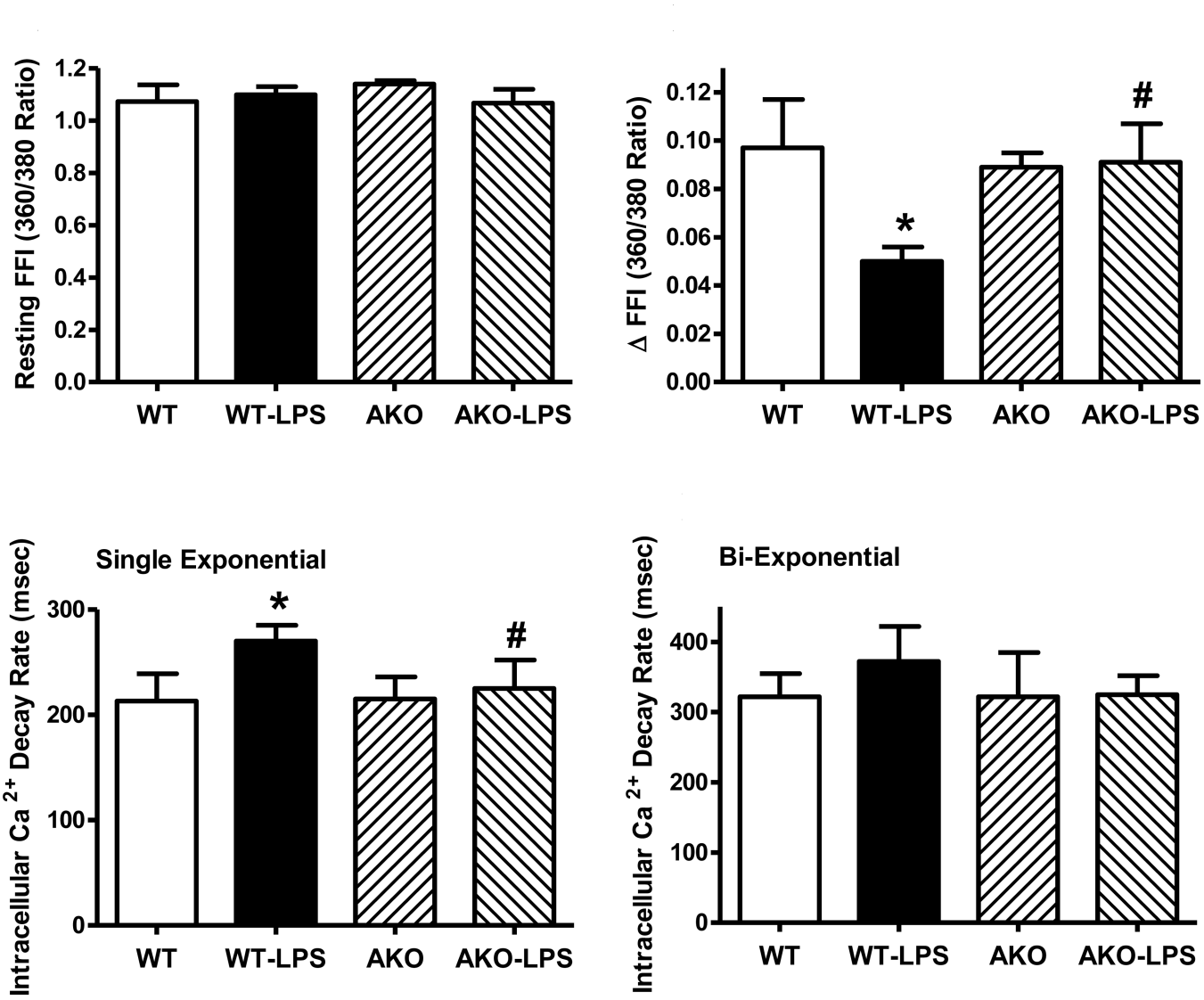

Fig. 2.

Cardiomyocyte intracellular Ca^{2+} properties in WT and Akt2 knockout (AKO) mice treated with LPS (4 mg/kg, i.p.) or saline for 4 hrs. A: Resting Fura-2 fluorescence intensity (FFI); B: Electrically-stimulated rise in FFI (ΔFFI); C: Intracellular Ca^{2+} decay rate (single exponential); D: Intracellular Ca^{2+} decay rate (bi-exponential). Mean ± SEM, n = 4 mice (20 cells per mouse) per group; * $p < 0.05$ *vs*. WT group, # $p < 0.05$ *vs*. WT-LPS group.

NIH-PA Author Manuscript
NIH-PA Author Manuscript
NIH-PA Author Manuscript

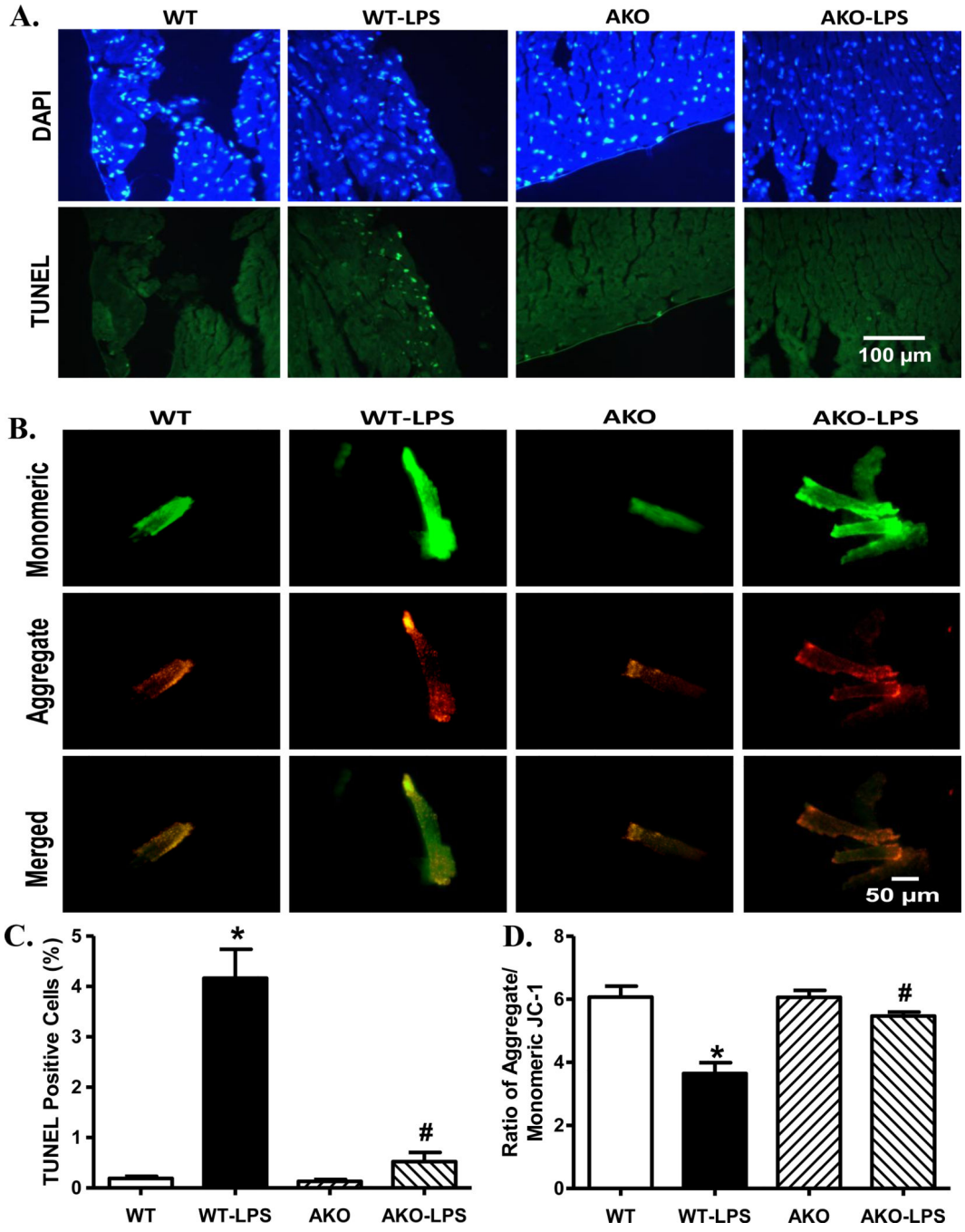

Fig. 3.

Assessment of myocardial apoptosis and cardiomyocyte mitochondrial membrane potential (MMP) using TUNEL staining and JC-1 fluorescence, respectively, from WT and Akt2 knockout mice treated with LPS (4 mg/kg, i.p.) or saline for 4 hrs. A: TUNEL staining. All nuclei were stained with DAPI (blue) and the TUNEL-positive nuclei were visualized with fluorescein (green). Original magnification = 400×, scale bar = 100 μm; B: MMP itochondrial membrane potential. Representative images of monomeric JC-1 staining of cardiomyocytes (top row), aggregate JC-1 staining (middle row); and merged images

(bottom row), scale bar= 50 μm; C: Quantitative analysis of TUNEL positive cells from 7–8 fields from 3 mice per group; and D: Quantitative analysis of red/green fluorescence ratio (5 mice per group). Mean ± SEM, * $p < 0.05$ *vs*. WT group, # $p < 0.05$ *vs*. WT-LPS group.

NIH-PA Author Manuscript
NIH-PA Author Manuscript
NIH-PA Author Manuscript

NIH-PA Author Manuscript
NIH-PA Author Manuscript
NIH-PA Author Manuscript

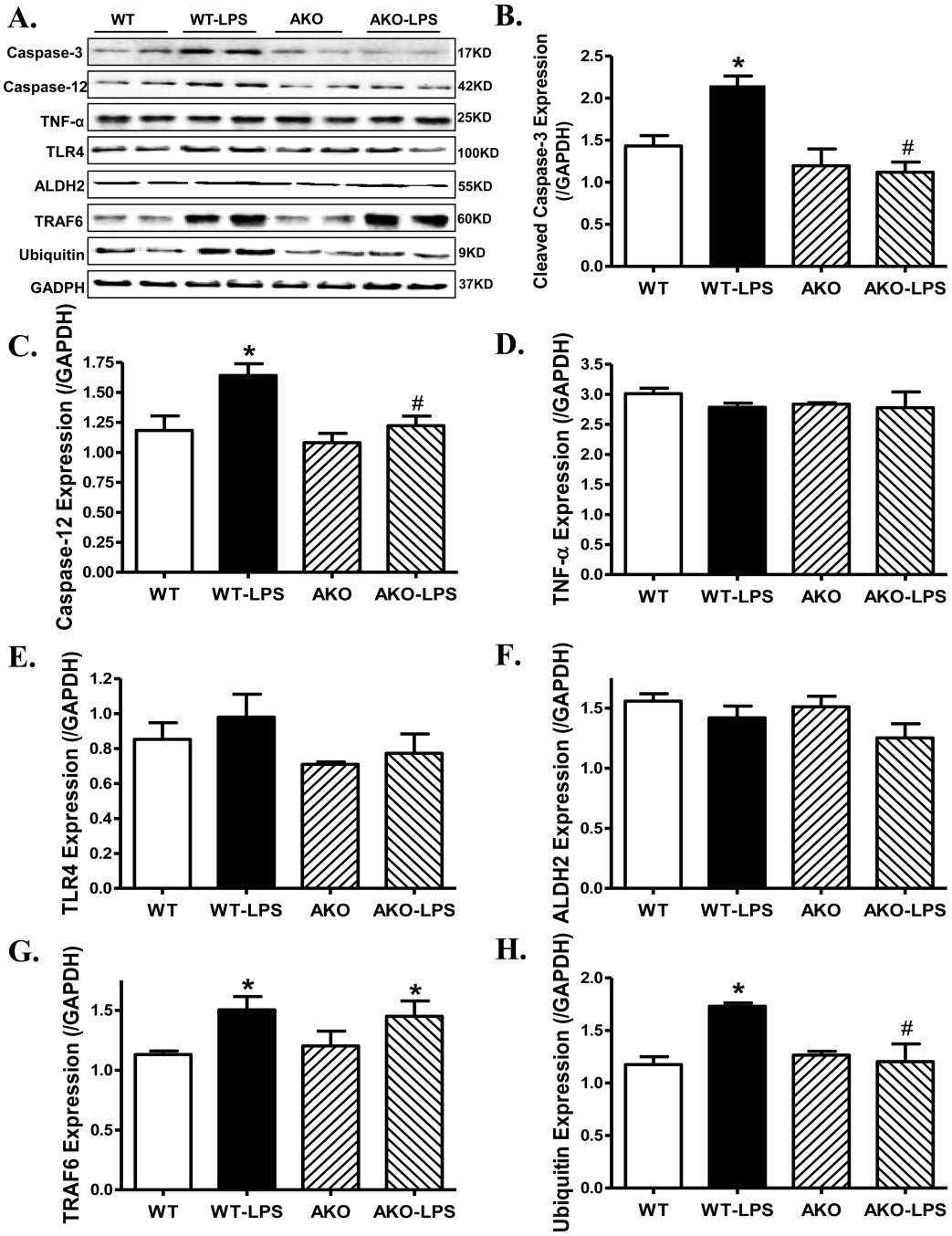

Fig. 4.

Western blot analysis of protein markers for apoptosis, inflammation, mitochondrial integrity and ubiquitination in myocardium from WT and Akt2 knockout (AKO) mice treated with LPS (4 mg/kg, i.p.) or saline for 4 hrs. A: Representative gel blots (2 mice per group were shown) depicting expression of Caspase-3, −12, TNF-α, TLR4, the mitochondrial protein ALDH2, the ubiquitin E3 ligase TRAF6 and ubiquitin (GAPDH was used as loading control) using specific antibodies; B: Cleaved caspase-3; C: Caspase-12; D: TNF-α; E: TLR4; F: ALDH2; G: TRAF6 and H: Ubiquitin; Mean ± SEM, n = 4 mice for

WT group and 6 mice per group for all other groups, * $p < 0.05$ *vs*. WT group, # $p < 0.05$ *vs*. WT-LPS group.

NIH-PA Author Manuscript
NIH-PA Author Manuscript
NIH-PA Author Manuscript

NIH-PA Author Manuscript
NIH-PA Author Manuscript
NIH-PA Author Manuscript

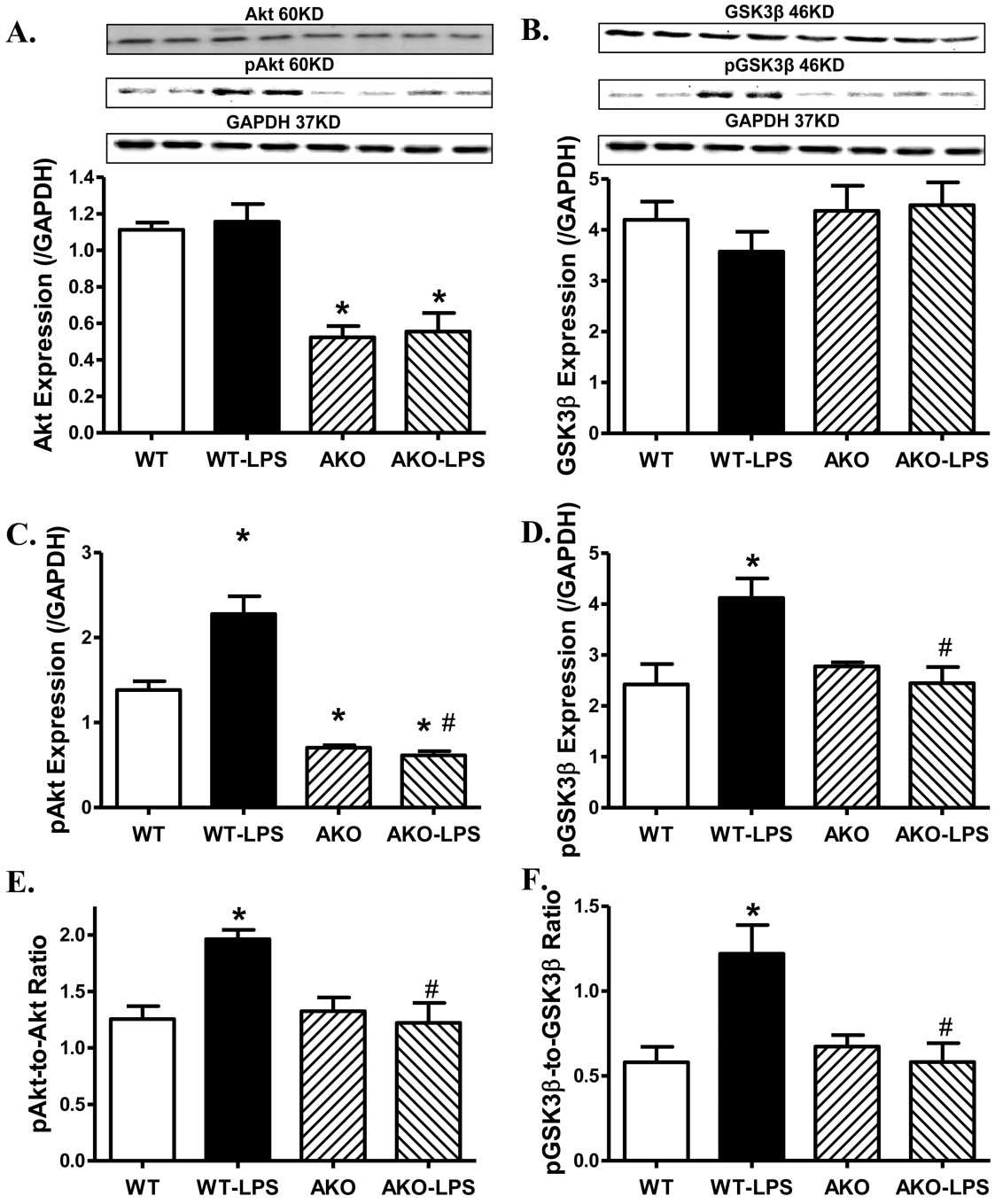

Fig. 5.

Western blot analysis of pan and phosphorylated Akt and GSK3β in myocardium from WT and Akt2 knockout (AKO) mice treated with LPS (4 mg/kg, i.p.) or saline for 4 hrs. A: Pan Akt; B: Pan GSK3β; C: Phosphorylated Akt (pAkt); D: Phosphorylated GSK3β (pGSK3β); E: pAkt-to-Akt ratio; and F: pGSK3β-to-GSK3β ratio; Insets: Representative gel blots (2 mice per group) depicting expression of pan or phosphorylated Akt and GSK3β (GAPDH used as loading control) using specific antibodies; Mean ± SEM, n = 5 mice for WT group

and 6 mice per group for all other groups, * $p < 0.05$ *vs*. WT group, # $p < 0.05$ *vs*. WT-LPS group.

NIH-PA Author Manuscript
NIH-PA Author Manuscript
NIH-PA Author Manuscript

NIH-PA Author Manuscript
NIH-PA Author Manuscript
NIH-PA Author Manuscript

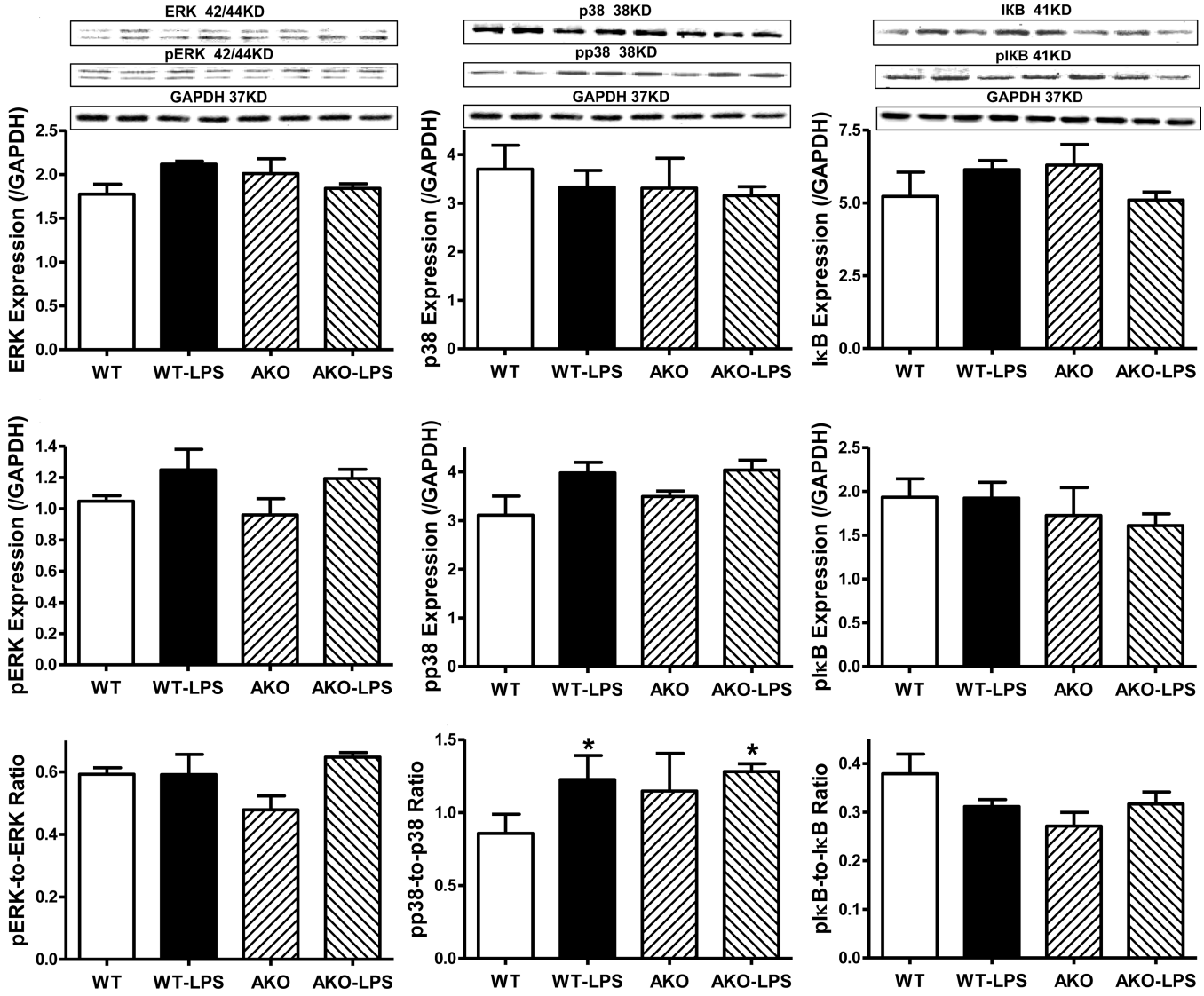

Fig. 6.

Western blot analysis of pan and phosphorylated ERK, p38 and IĸB in myocardium from WT and Akt2 knockout (AKO) mice treated with LPS (4 mg/kg, i.p.) or saline for 4 hrs. A: Pan ERK; B: Pan p38; C: pan IĸB; D: Phosphorylated ERK (pERK); E: Phosphorylated p38 (pp38); F: Phosphorylated IĸB; G: pERK-to-ERK ratio; H: pp38-to-p38 ratio; and I: pIĸB-to-IĸB ratio; Insets: Representative gel blots (2 mice per group) depicting expression of pan and phosphorylated ERK, p38 and IĸB (GAPDH used as loading control) using specific antibodies; Mean ± SEM, n = 3 per group for WT group and 4 mice per group for all other groups, * $p < 0.05$ *vs*. WT group, # $p < 0.05$ *vs*. WT-LPS group.

NIH-PA Author Manuscript
NIH-PA Author Manuscript
NIH-PA Author Manuscript

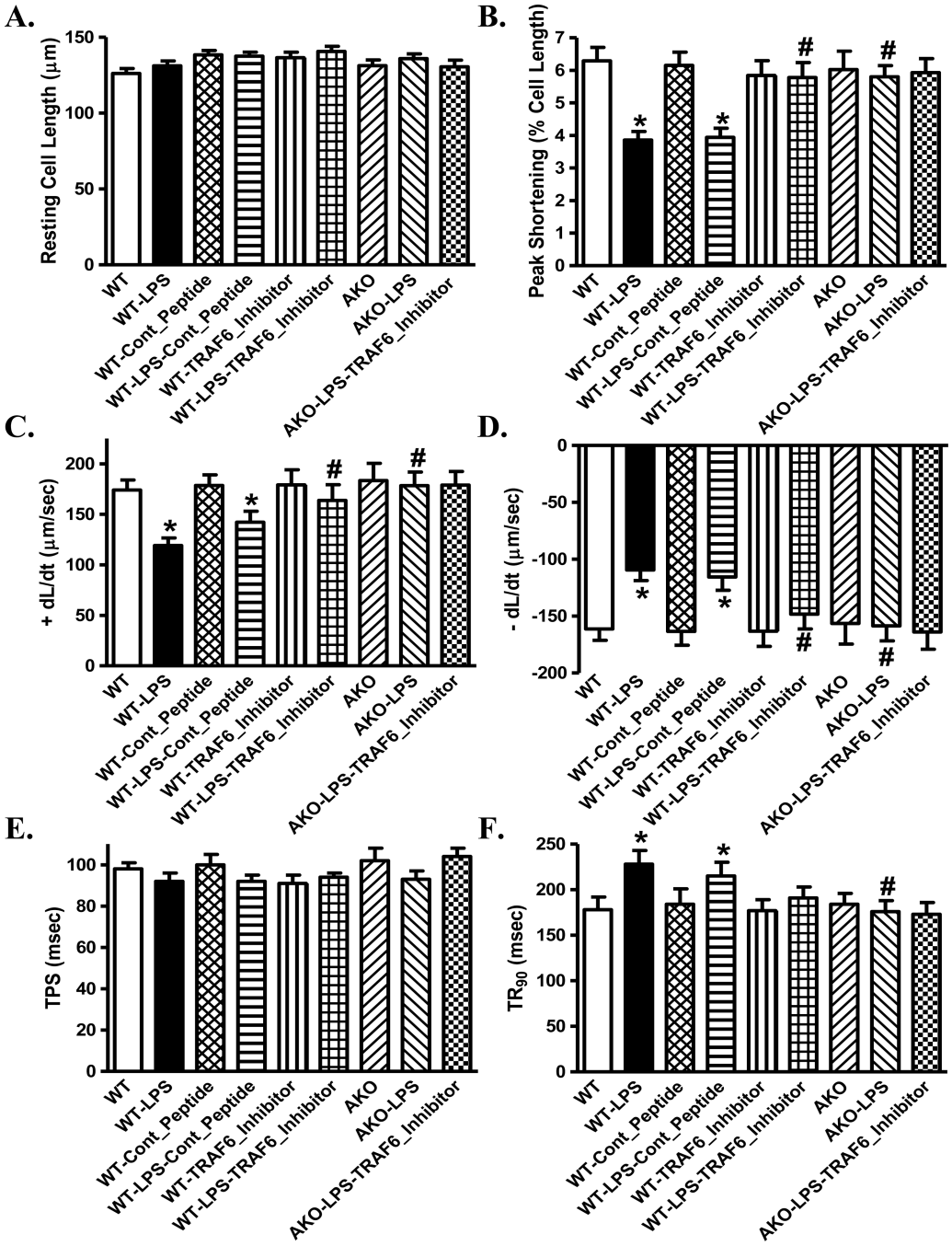

Fig. 7.

Effect of the TRAF6 inhibitory peptide and control peptide on lipopolysaccharide (LPS)-induced cardiomyocyte contractile defects. Freshly isolated cardiomyocytes from WT or akt2 knockout (AKO) mice were incubated with LPS (1 μg/ml) in the presence or absence of TRAF6 inhibitory peptide (300 μM) or control peptide (300 μM) for 4 hrs. A: Resting cell length; B: Peak shortening (normalized to resting cell length); C: Maximal velocity of shortening (+ dL/dt); D: Maximal velocity of relengthening (− dL/dt); E: Time-to-peak

shortening (TPS) and F: Time-to-90% relengthening (TR_{90}). Mean ± SEM, n = 62 cells per group, * $p < 0.05$ *vs*. WT group, # $p < 0.05$ *vs*. WT-LPS group.

NIH-PA Author Manuscript
NIH-PA Author Manuscript
NIH-PA Author Manuscript

NIH-PA Author Manuscript

NIH-PA Author Manuscript

NIH-PA Author Manuscript

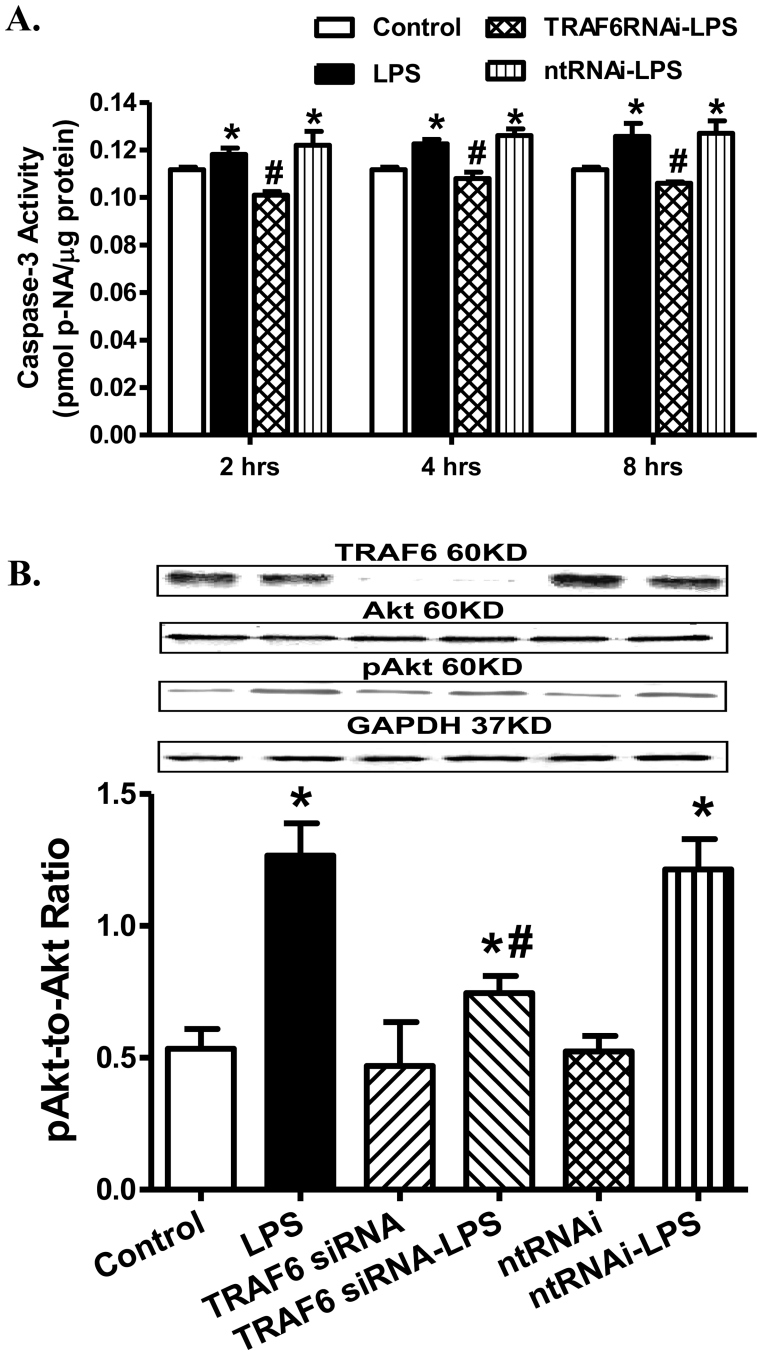

Fig. 8.

Effect of TRAF6 silencing (for 96 hrs) on lipopolysaccharide (LPS, 100 μM)-induced apoptosis and Akt phosphorylation in H9C2 myoblasts. Non-target RNAi (ntRNAi) was used as negative control. A: Apoptosis measured using caspase-3 activity at 2- 4- and 8-hrs after LPS challenge; and B: pAkt-to-Akt following TRAF6 siRNA or ntRNAi and 4 hrs of LPS treatment. Insets: Representative gel blots depicting expression of TRAF6, pan and phosphorylated Akt (GAPDH was used as loading control) using specific antibodies; Mean ± SEM, n = 4 independent cultures, * $p < 0.05$ *vs*. control group, # $p < 0.05$ *vs*. LPS group.

NIH-PA Author Manuscript
NIH-PA Author Manuscript
NIH-PA Author Manuscript

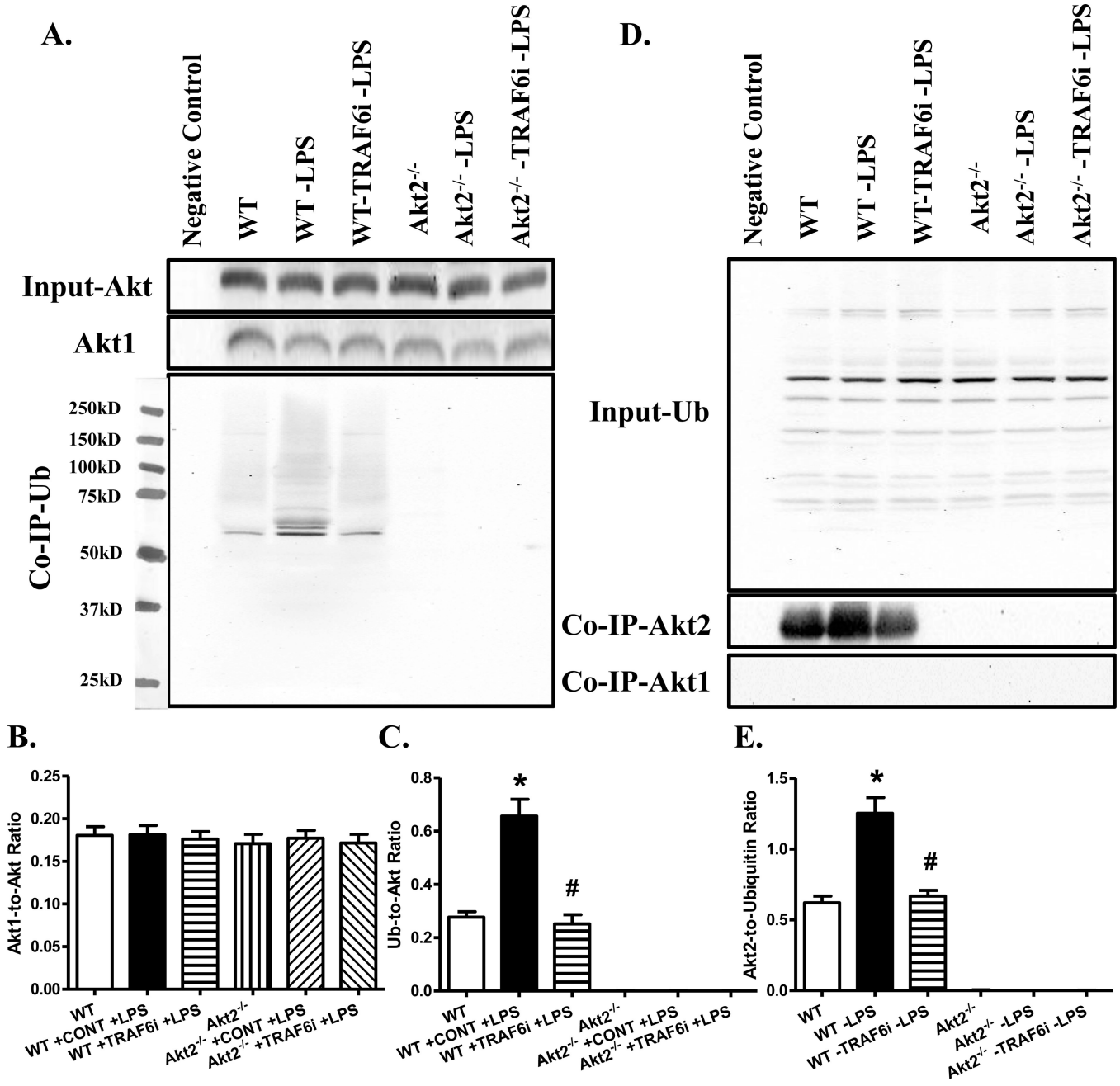

Fig. 9.

Role of TRAF6 and Akt2 in LPS-induced Akt ubiquitination. Cardiomyocytes from WT and Akt2 knockout mice were challenge with LPS (1 μg/ml) for 4 hrs in the absence or presence of the TRAF6 peptide inhibitor or control peptide (300 μM) prior to immunoblotting analysis. A: Cardiomyocyte samples from WT and Akt2$^{-/-}$ mice were immunoprecipitated with the anti-pan Akt antibody. Akt1 and ubiquitin levels were detected using western blotting. Pan Akt was used as the input and ubiquitin was pulled down with pan Akt and detected by western blotting. Akt1 level was also examined in the protein extract pulled down by pan Akt. AminoLink Plus coupling resin uncoupled with the pan Akt antibody was

NIH-PA Author Manuscript

NIH-PA Author Manuscript

NIH-PA Author Manuscript

employed as the negative control. B: Quantitative analysis of Akt1 levels in protein extracts pulled down by pan Akt; C: Quantitative analysis of ubiquitinated protein (Ub) pulled down with pan Akt; D: Cardiomyocyte samples from WT and Akt2$^{-/-}$ mice were immunoprecipitated with the anti-ubiquitin antibody. Ubiquitin was employed as the input; Akt2 and Akt1 protein levels were detected using western blotting. AminoLink Plus coupling resin uncoupled with the ubiquitin antibody was used as the negative control; and E: Quantitative analysis of Akt2 protein precipitated with ubiquitin. Mean ± SEM, n = 4–5 mice per group, * $p < 0.05$ *vs*. WT group, # $p < 0.05$ *vs*. WT-LPS group.

NIH-PA Author Manuscript

NIH-PA Author Manuscript

NIH-PA Author Manuscript

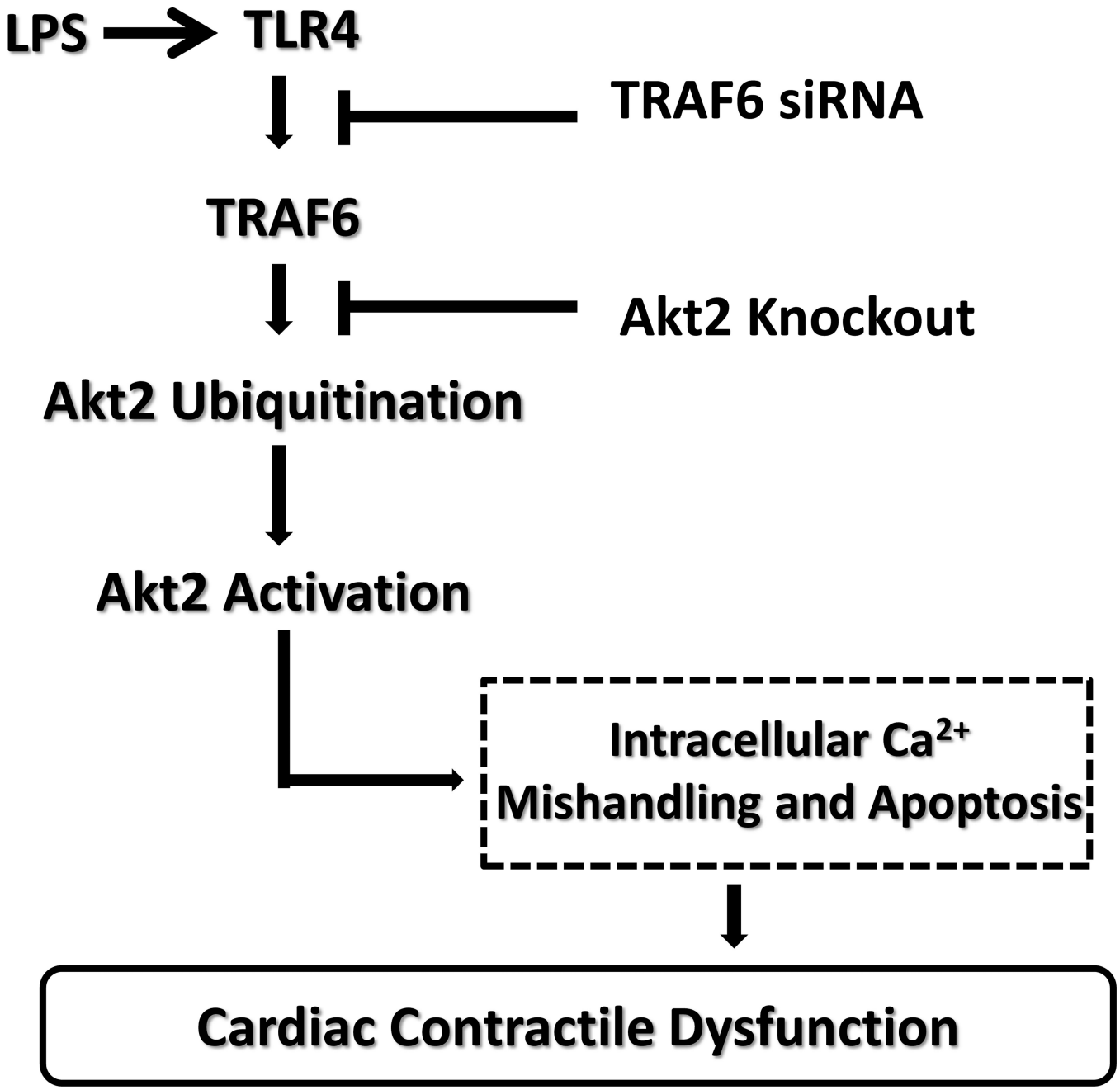

Fig. 10.

Schematic diagram depicting the proposed signaling mechanism behind LPS- and Akt2 knockout-induced myocardial contractile responses. TLR4: toll-like receptor 4; TRAF6: TNF receptor-associated factor 6.

NIH-PA Author Manuscript

NIH-PA Author Manuscript

NIH-PA Author Manuscript

Table 1

Biometric and echocardiographic parameters of WT and Akt2 knockout (AKO) mice with or without LPS challenge (4 mg/kg, i.p., for 4 hrs)

Parameter	WT (9)	WT-LPS (9)	AKO (8)	AKO-LPS (8)
Body Weight (g)	27.2 ± 0.9	26.1 ± 1.1	27.4 ± 1.0	28.2 ± 0.4
Heart Weight (mg)	158 ± 4	155 ± 5	165 ± 5	164 ± 4
Heart/Body Weight (mg/g)	5.85 ± 0.17	5.97 ± 0.11	6.06 ± 0.28	5.82 ± 0.18
Liver Weight (g)	1.36 ± 0.03	1.36 ± 0.05	1.37 ± 0.03	1.38 ± 0.03
Liver/Body Weight (mg/g)	50.4 ± 1.7	52.3 ± 2.1	50.5 ± 2.0	49.2 ± 1.4
Kidney Weight (mg)	361 ± 9	352 ± 7	358 ± 4	364 ± 7
Kidney/Body Weight (mg/g)	13.3 ± 0.2	13.6 ± 0.5	13.2 ± 0.5	12.9 ± 0.3
Diastolic BP (mmHg)	84.5 ± 2.9	79.8 ± 3.4	79.3 ± 3.1	82.5 ± 2.6
Systolic BP (mmHg)	112.2 ± 1.6	109.5 ± 3.1	110.3 ± 3.6	110.7 ± 3.7
Heart Rate (bpm)	478 ± 32	466 ± 33	466 ± 35	442 ± 18
Wall Thickness (mm)	1.00 ± 0.14	0.97 ± 0.11	0.99 ± 0.06	1.01 ± 0.05
LVEDD (mm)	2.15 ± 0.10	2.10 ± 0.21	2.25 ± 0.14	2.27 ± 0.11
LVESD (mm)	1.12 ± 0.07	1.44 ± 0.07*	1.19 ± 0.10	1.19 ± 0.05#
Calculated LV Mass (mg)	71.4 ± 7.4	63.0 ± 13.5	64.9 ± 7.3	64.7 ± 8.4
Fractional Shortening (%)	48.6 ± 1.8	32.4 ± 3.1*	44.3 ± 3.3	47.6 ± 2.5#

BP = blood pressure; LVEDD = left ventricular end diastolic diameter; LVESD = left ventricular end systolic diameter. Mean ± SEM, sample size is given in parentheses,

* $p < 0.05$ *vs.* WT group,

# $p < 0.05$ *vs.* WT-LPS group.